International Journal of Solids and Structures 144–145 (2018) 46–58

Contents lists available at ScienceDirect

International Journal of Solids and Structures

journal homepage: www.elsevier.com/locate/ijsolstr

On micromechanical modeling of orthotropic solids with parallel cracks

K. Vasylevskyi [a], B. Drach [b], I. Tsukrov [a,*]

[a] Department of Mechanical Engineering, University of New Hampshire, Durham, NH 03824, USA
[b] Department of Mechanical & Aerospace Engineering, New Mexico State University, Las Cruces, NM 88003, USA

ARTICLE INFO

Article history:
Received 15 August 2017
Revised 3 January 2018
Available online 30 April 2018

Keywords:
Homogenization
Penny-shaped cracks
Orthotropic matrix
Micromechanical models
Periodic RVEs

ABSTRACT

A detailed comparison of the accuracy of several popular micromechanical schemes utilized for prediction of the effective elastic properties of materials with parallel cracks is presented. In particular, the non-interaction, Mori–Tanaka, differential and self-consistent schemes are compared against the direct finite element simulations. The latter are performed on the periodic representative volume elements containing 30 strongly oblate spheroids representing the penny-shaped cracks. This work extends the existent results to a more general class of matrix materials – orthotropic materials, which requires the ability to calculate the Eshelby tensor for an ellipsoid in non-isotropic matrix. In addition to the implementation of the integration procedure used for the Eshelby tensor calculation, this work also presents a variation of the Random Sequential Adsorption algorithm modified for periodic structures.

Analysis of the results indicates that in the case of parallel nearly flat cracks (strongly oblate spheroids) the overall out-of-plane moduli are best predicted by the differential scheme. On the other hand, Mori–Tanaka scheme should be used for estimation of the in-plane moduli. It also appears that as the cracks are inflated from strongly oblate spheroids to slightly deformed spheres, the best choice of the micromechanical scheme for the out-of-plane properties gradually shifts towards Mori–Tanaka.

1. Introduction

Micromechanical schemes, based on certain simplifying assumptions with respect to interaction of inhomogeneities, provide an efficient tool to predict the overall (effective) elastic properties of materials with inhomogeneities (Mori and Tanaka, 1973; Benveniste, 1987; Kröner, 1958; Hill, 1965; Budiansky, 1965; McLaughlin, 1977; Salganik, 1973; Eroshkin and Tsukrov, 2005). They are particularly suited for parametric studies focusing on evaluation of the effects of inhomogeneities shapes, concentration, and stiffness or compliance on the overall response. For such parametric studies, direct numerical simulations of a large number of the representative volume elements (RVE) of the materials with inhomogeneities would require significant computational resources and are not always feasible. Note that the third popular micromechanical approach involving establishing exact variational bounds on the overall elastic properties (Hashin and Shtrikman, 1963) may result in the bounds that are too wide in the case of large contrast in the elastic properties of matrix and inhomogeneities, e.g. pores and cracks.

In this paper we investigate the accuracy of several popular micromechanical schemes for isotropic and orthotropic solids with parallel penny-shaped cracks. This is done by comparing the analytical micromechanical modeling results with direct finite element (FE) simulations conducted on the RVEs of the cracked solids. We also consider how the accuracy of the schemes changes if the cracks in the solids are “inflated” to become the oblate spheroidal pores.

Evaluation of contribution of cracks to the effective elastic properties of cracked solids is one of the classical and well developed topics in the mechanics of solids, as reviewed, for example, in Kachanov (1993). However, certain controversy exists in the choice of the best micromechanical modeling approach to this problem, in particular, Mori–Tanaka (MT) (Mori and Tanaka, 1973; Benveniste, 1987) or differential (DIFF) scheme (Salganik, 1973; McLaughlin, 1977; Zimmerman, 1985). Note that in the case of cracks the predictions of Mori–Tanaka approach coincide with the non-interaction (NI) approximation, see Kachanov (1993). A number publications argue in favor of NI (and hence MT) scheme, see Kachanov (1993), Kachanov et al., (1994) and Grechka and Kachanov (2006). Their conclusions are based on comparison with

* Corresponding author.
E-mail addresses: kv1012@wildcats.unh.edu (K. Vasylevskyi), borys@nmsu.edu (B. Drach), igor.tsukrov@unh.edu (I. Tsukrov).

https://doi.org/10.1016/j.ijsolstr.2018.02.038
0020-7683/

numerical results utilizing the "transmission factors" approach of Kachanov (1987) or finite element simulations. On the other hand, in studies of several other research groups (Dahm and Becker, 1998; Orlowsky et al., 2003; Saenger et al., 2006) the differential scheme was found to be closer to numerical results. Saenger (2007) claimed that the results of Grechka (2007) favor the non-interaction approximation over differential scheme due to unjustified constraints on the location of cracks within RVE. Seelig et al. (2000) implemented the "transmission factor" approach of Kachanov (1987) in combination with the boundary element method. Their numerical results for random and parallel 2D cracks are located between the NI and DIFF predictions.

All of the above publications deal with cracks in isotropic matrices. For anisotropic solids with cracks, Gottesman et al. (1980) considered influence of parallel cracks on a fibrous composite material on the basis of variational techniques and also in the self-consistent scheme framework. Laws et al. (1983) presented results for transversely isotropic material with parallel cracks infinitely long in the direction of transverse isotropy axis (plane strain formulation). The cracks were modeled as elliptical cylinders; the results were obtained using self-consistent method. Hashin (1988) considered isotropic material with randomly oriented cracks and 2D case of orthotropic material with parallel cracks utilizing differential and self-consistent methods. Deng and Nemat-Nasser (1992) considered anisotropic material with parallel cracks in 2D using dilute distribution, differential and self-consistent methods. Mauge and Kachanov (1994) performed numerical simulations on sample arrays of parallel and randomly oriented interacting cracks in 2D materials with random anisotropy and compared the calculated values of Young's moduli with predictions given by non-interaction, self-consistent and differential schemes. Their simulations were limited by the requirement that neighboring cracks were not closer than 0.2 of crack lengths to have convergence in the utilized numerical procedure.

3D results for anisotropic matrix are mostly limited to transversely isotropic materials with cracks parallel to the plane of isotropy. Willis (1977) presented expressions for Hashin–Shtrikman bounds and self-consistent approach for composite with anisotropic constituents and illustrated the results by calculating the effective conductivity of an anisotropic matrix with aligned spheroidal inhomogeneities. Withers (1989) derived a solution for elastic fields around an ellipsoidal inclusion in transversely isotropic matrix using a method analogous to Eshelby (1957). Kushch and Sevostianov (2004) presented results for effective elastic properties of composites with spherical inhomogeneities and transversely isotropic material properties obtained using an analytical approach based on the multipole expansion method. Sevostianov et al. (2005) performed a micromechanical modeling based on the stiffness and compliance contribution tensors combined with non-interaction and effective field method for composites with spheroidal inhomogeneities and transversely isotropic phases.

In this paper we investigate the applicability of several commonly used micromechanical schemes to prediction of effective elastic response of orthotropic materials containing parallel penny-shaped crack-like pores. The paper is organized as follows. Section 2 presents our approach to micromechanical modeling based on contribution of a single inhomogeneity to the effective elastic properties combined with non-interaction, Mori–Tanaka, differential and self-consistent schemes. The procedures for geometry generation, meshing, FE model preparation and processing of simulation results are described in section 3. This section includes a mesh sensitivity study, in which we compare the effect of two mesh refinement techniques (local and global) and the order of the volumetric finite elements on the elastic moduli predictions. Section 4 focuses on the performance of the micromechanical schemes for orthotropic materials containing parallel crack-like pores. The section also contains a validation of the numerical procedure for calculating the Eshelby tensor for orthotropic materials which is required for the proposed micromechanical modeling. Section 5 presents a study on the accuracy of the considered micromechanical schemes for isotropic materials with oblate spheroidal pores having aspect ratios in the range 0.1–0.8. Final conclusions of this research are formulated in Section 6.

2. Micromechanical modeling

The micromechanical approach utilized in this paper is based on the compliance contribution tensor of inhomogeneities **H**. This concept was first introduced in Horii and Nemat-Nasser (1983) and then used in Kachanov et al. (1994) to evaluate contributions of various pores in isotropic 2D and 3D materials. The approach is presented here for materials with inhomogeneities of general type and shape following Eroshkin and Tsukrov (2005). In the case of pores and cracks the stiffness of the inhomogeneity is equal to zero.

In this work we assume that the cracked material is statistically homogenous and a certain representative volume element (RVE) can be chosen such that its properties are the same as of the entire heterogeneous material. More detail on the concept of the RVE can be found in Hill (1963) and Markov (1999).

The effective compliance **S** of a material with inhomogeneities is expressed as

$$\mathbf{S} = \mathbf{S}_{\mathrm{M}} + \mathbf{H}^{\mathrm{RVE}}, \tag{1}$$

where $\mathbf{S}_{\mathrm{M}}$ is the compliance tensor of the matrix material and $\mathbf{H}^{\mathrm{RVE}}$ is the compliance contribution tensor of all inhomogeneities present in the RVE. For non-interacting defects tensor $\mathbf{H}^{\mathrm{RVE}}$ can be found simply as a sum of contributions of individual defects. The approaches to deal with interacting defects are discussed later in this section.

In order to obtain contributions of various types of defects, we need to solve the so-called "single inclusion problem". Contribution of an inhomogeneity to the overall properties of a material is evaluated as follows. The inhomogeneity of volume V_{I} is placed in an infinite elastic matrix subjected to the remotely applied stress $\boldsymbol{\sigma}^{\infty}$. The additional average strain in some reference volume $\tilde{V}$ containing inhomogeneity is proportional to the applied stress:

$$\Delta\boldsymbol{\varepsilon} = \mathbf{H} : \boldsymbol{\sigma}^{\infty}$$

where **H** is the inhomogeneity compliance contribution tensor.

Most of the micromechanical models are based on the solution for the ellipsoidal inhomogeneity provided by Eshelby (1957). Originally the solution was derived for the isotropic material in terms of elliptic integrals for a general ellipsoidal inhomogeneity. Later this solution was expanded to other types of matrix material symmetry, see, for example, Sevostianov et al. (2005). However, there is still no explicit analytical solution of the Eshelby problem for a general anisotropic material. This issue was addressed by Mura (1987), who proposed to simplify the elliptic integrals to triple integrals. The idea was implemented numerically by Ghahremani (1977) and improved by Gavazzi and Lagoudas (1990).

The expression for the compliance contribution tensor of an ellipsoidal inclusion **H** in terms of the compliance tensors of the matrix $\mathbf{S}_{\mathrm{M}}$ and the inhomogeneity $\mathbf{S}_{\mathrm{I}}$ and Eshelby tensor **s** can be written as (see Sevostianov and Kachanov, 2002)

$$\mathbf{H} = \frac{V_{\mathrm{I}}}{\tilde{V}}\left[(\mathbf{S}_{\mathrm{I}} - \mathbf{S}_{\mathrm{M}})^{-1} + \mathbf{S}_{\mathrm{M}}^{-1} : (\mathbf{I} - \mathbf{s})\right]. \tag{2}$$

It is extremely difficult to analytically solve the elasticity problem for multiple interacting inhomogeneities. So, the interaction between defects is taken into account utilizing various simplifying micromechanical models (or schemes). Depending on how

we treat the interaction between the inhomogeneities various micromechanical models are distinguished.

2.1. Non-interaction micromechanical model

This scheme is based on the assumption that separate inhomogeneities do not interact with each other. In this case, the combined compliance contribution tensor of the entire RVE is calculated as a sum of the individual inhomogeneities' contributions

$$\mathbf{H}^{\mathrm{NI}} = \sum^{\mathbf{H}}, \ \mathbf{S} = \mathbf{S}_{\mathrm{M}} + \mathbf{H}^{\mathrm{NI}} \tag{3}$$

where $\mathbf{H}^{\mathrm{NI}}$ is the $\mathbf{H}^{\mathrm{RVE}}$ for the non-interacting inhomogeneities

2.2. Mori–Tanaka micromechanical model

This model assumes that inhomogeneity is subjected to the remotely applied stress $\boldsymbol{\sigma}_{\mathrm{M}}$ which is equal to the average stress within the matrix phase of the RVE, see Mori and Tanaka (1973) and Benveniste (1987). Mathematically it can be written as

$$\mathbf{H}^{\mathrm{MT}} = \mathbf{H}^{\mathrm{NI}} : \left[f_{\mathrm{M}}(\mathbf{S_I} - \mathbf{S_M}) + \mathbf{H^{NI}}\right]^{-1} : (\mathbf{S_I} - \mathbf{S_M}), \tag{4}$$

$$\mathbf{S} = \mathbf{S}_{\mathrm{M}} + \mathbf{H}^{\mathrm{NI}},$$

where f_{M} is the volume fraction of the matrix material.

2.3. Self-consistent micromechanical model

This approximation is based on the assumption that each inhomogeneity is subjected to the remotely applied stress and placed into the matrix material with the properties equivalent to the overall effective properties of the inhomogeneous material (Kröner, 1958; Hill, 1965; Budiansky, 1965). The effective compliance tensor of this material is found from the transcendent equation:

$$\mathbf{S} = \mathbf{S}_M + (\mathbf{S_I} - \mathbf{S_M}) : (\mathbf{S_I} - \mathbf{S})^{-1} : \mathbf{H}^{\mathrm{NI}}(\mathbf{S}, \mathbf{S}_{\mathrm{I}}), \tag{5}$$

where $\mathbf{H}^{\mathrm{NI}}(\mathbf{S},\mathbf{S}_{\mathrm{I}})$ is the non-interaction $\mathbf{H}$-tensor of the RVE calculated for the matrix material having the effective compliance. In general case, Eq. (5) doesn't have an analytical solution and can only be solved numerically.

2.4. Differential micromechanical model

The idea of this model is in incrementally increasing the volume fraction of the inhomogeneities until the desired value is reached. At each iteration the non-interaction inhomogeneity problem is solved for the matrix having the compliance of the homogenized material (Salganik, 1973; McLaughlin, 1977). Mathematically, this model is represented as the following ordinary differential equation

$$\frac{d\mathbf{S}}{dt} = \frac{1}{f_{\mathrm{I}}(1-t)}\mathbf{H}^{\mathrm{NI}}(\mathbf{S}(t), \mathbf{S}_{\mathrm{I}}), \ \mathbf{S}(0) = \mathbf{S}_{\mathrm{M}} \tag{6}$$

or

$$\frac{\mathrm{d}\mathbf{H}^{\mathrm{DIFF}}}{\mathrm{dt}} = \frac{1}{\mathrm{f_I}(1-t)}\mathbf{H}^{\mathrm{NI}}\left(\mathbf{S}_{\mathrm{M}} + \mathbf{H}^{\mathrm{DIFF}}, \mathbf{S}_{\mathrm{I}}\right), \ \mathbf{H}^{\mathrm{DIFF}}(0) = 0, \tag{7}$$

where t is the integration variable which changes in the range [0, f_{I}], where f_{I} is the volume fraction of inhomogeneities.

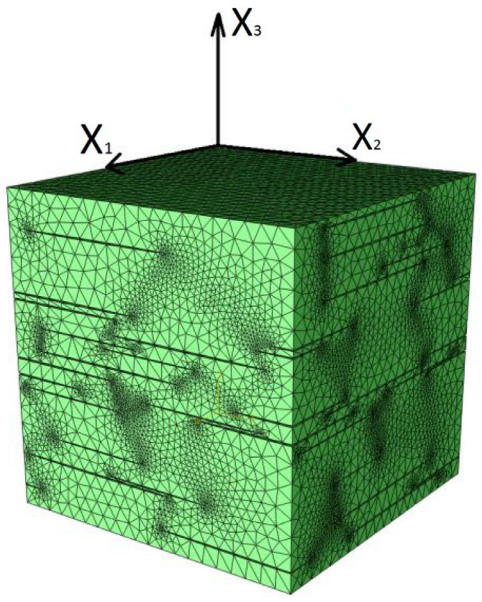

Fig. 1. RVE containing parallel cracks and meshed with 3D elements; crack density (as defined by formula (8)) is $\rho = 0.7$.

3. Numerical simulations

3.1. Generation of the RVE

Numerical predictions of effective elastic properties of a cracked solid were obtained by finite element analysis of periodic RVEs with multiple cracks. Each RVE contained 30 identical randomly distributed parallel cracks that were approximated by penny-shaped (spheroidal) pores having semi-axes $a_1 = a_2 = R$, $a_3 = \alpha R$, where α is the spheroid's aspect ratio defining the thickness (opening) of the crack. Note that the overall elastic response of the cracked solid is less sensitive to the crack thickness than the stress concentrations (in the limiting case, stress intensity) near the crack tip. That is why the choice of α was mostly dictated by FE meshing convenience. In our simulations we assume $\alpha = 0.01$ (compare with $\alpha = 0.08$ in Grechka, 2007). The RVEs were subjected to prescribed displacements with the corresponding periodicity constraints. The effective stiffness was determined by relating the average stress in the RVE to the prescribed strain.

The following requirements had to be satisfied during generation of RVEs for this numerical study:

- the RVE must be suitable for the FE discretization,
- the RVE must be periodic (opposite faces of the unit cell are identical),
- the pores in the RVE have to be randomly distributed.

In the simulation, the RVE was assumed to be of a cubic shape and unit volume. The radii and aspect ratios of the pores were chosen based on the desired pore volume fraction (or crack density). To make the unit cell suitable for the finite element discretization, the distance between the neighboring pores had to be sufficient to avoid distorted finite elements. We constrained the distance between the neighboring pores to exceed 1/10th of the pore radius.

Periodic unit cells with 30 pores were generated using the Random Sequential Adsorption (RSA) algorithm (see Rintoul and Torquato, 1997). In the beginning, a single pore is inserted into the RVE and the coordinates of its center are stored, then it is checked if this pore intersects the faces of the RVE. If there is an intersection, the algorithm calculates the coordinates of the additional pores intersecting the opposite faces of the unit cell to keep it pe-

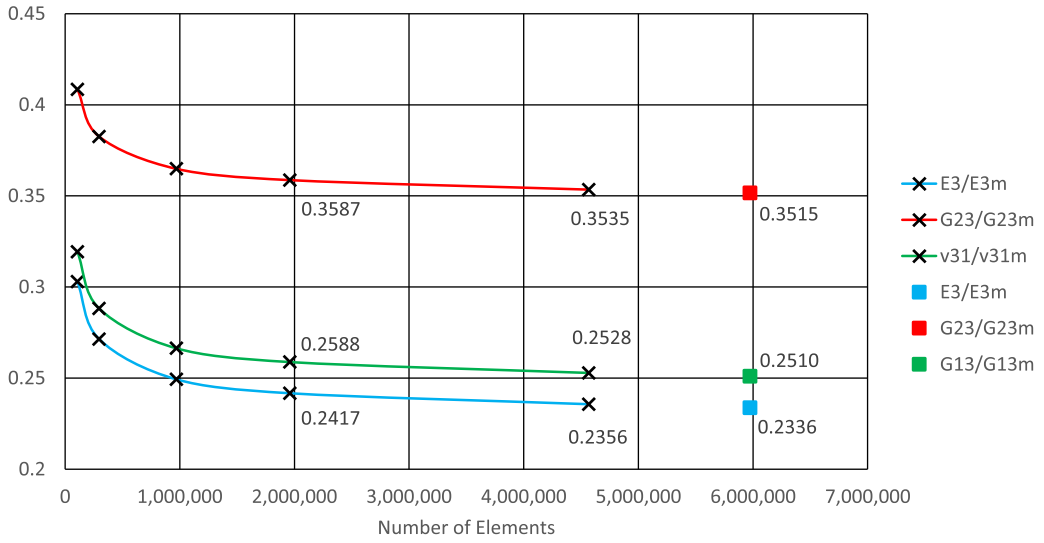

Fig. 2. Predictions of the effective E_3, G_{23} and ν_{31} as functions of number of elements. Symbol "■" denotes the result for the uniform mesh with 6 million elements.

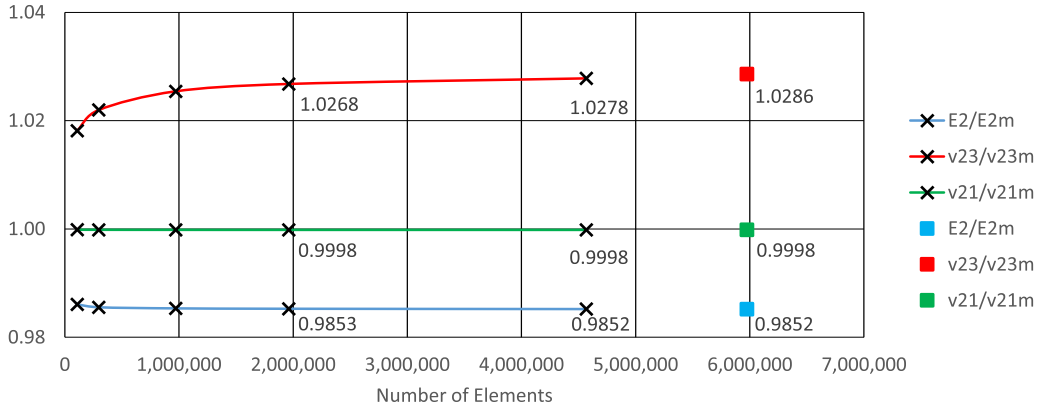

Fig. 3. Predictions of the effective E_2, ν_{21} and ν_{23} as functions of number of elements. Symbol "■" denotes the result for the uniform mesh with 6 million elements.

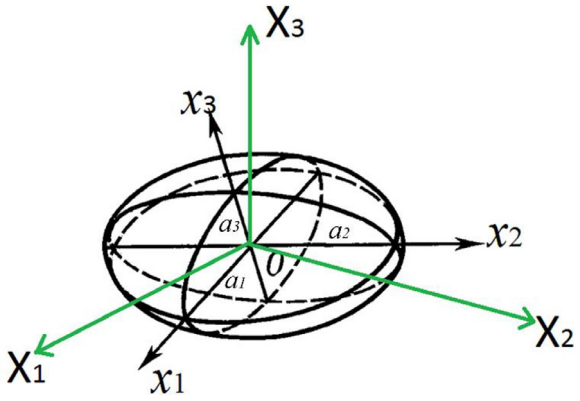

Fig. 4. General type ellipsoidal inhomogeneity in an orthotropic material with material symmetry axes $\mathbf{X}_1$, $\mathbf{X}_2$, $\mathbf{X}_3$.

riodic. The number and locations of the additional pores depend on the number of faces of the unit cell intersected by the initial pore. After the additional pores are added (if required), the coordinates of the next pore are produced by a random number generator following the uniform distribution. Then the algorithm checks if the newly added pore intersects the faces of the RVE cube; if it does then the corresponding additional pores required for periodicity are created. Next the algorithm checks if any of the newly added pores intersect the existing ones. In case of interpenetration, the newly generated pore (and the corresponding additional pores) are discarded. If there is no interpenetration then the coordinates of the centers of the new pores are stored and the process is continued until the desired porosity (or crack density) is achieved.

Once the final pore distribution is generated, the pore centers are imported into Abaqus software (see https://www.3ds.com/products-services/simulia/products/abaqus/) for generation of the geometric entities based on the data from the RSA algorithm and meshing of the unit cell. A custom Python (see https://www.python.org/) script was developed for the purpose of creating the geometric entities within the unit cube from an external file containing pore centers and dimensions.

When the geometry is generated, the surfaces of the pores are meshed with triangular surface finite elements. Note that the meshes on the opposite sides of the cube must be "congruent" (the mesh patterns must be identical) to make application of the periodic boundary conditions possible. For this purpose, the meshes from three orthogonal faces of the cube are duplicated to the opposite ones. The 3D mesh consisting of tetrahedral elements is generated based on the surface mesh using the "tri-to-tet" Abaqus meshing procedure. When the mesh is completed it is exported as a Marc Mentat (see http://www.mscsoftware.com/product/marc/) input file for further FEA analysis. An example of the mesh for the RVE with parallel cracks having crack density $\rho = 0.7$ is shown in

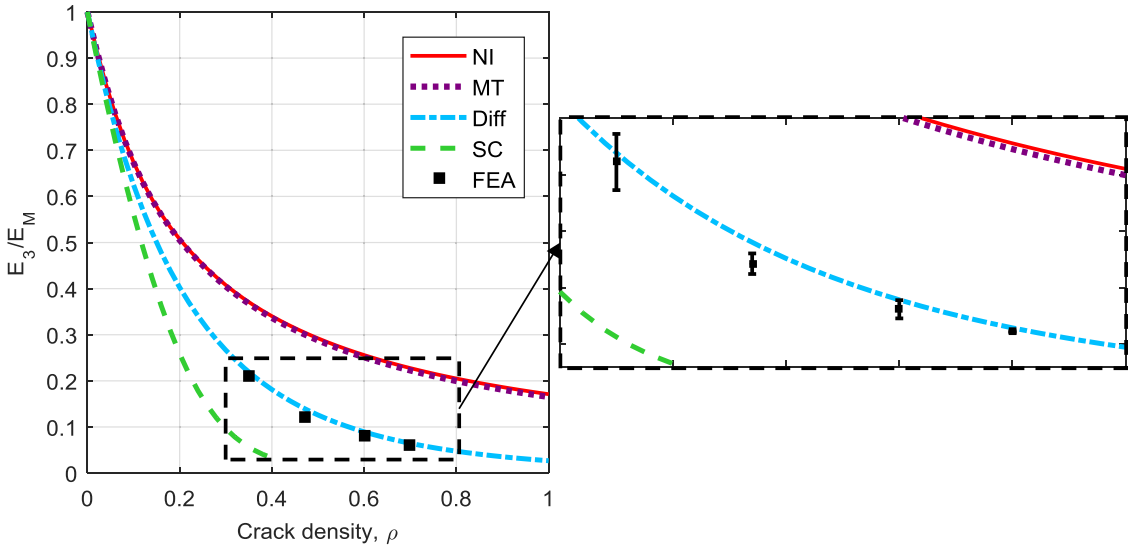

Fig. 5. Out-of-plane Young's modulus for orthotropic material with parallel cracks.

Fig. 1, where crack density ρ is defined as

$$\rho = \frac{\sum_{i=1}^{n} R_i^3}{V^{RVE}}. \tag{8}$$

Note that predictions of effective elastic properties of materials with pores and cracks are traditionally presented either as functions of crack density ρ or pore volume fraction (porosity)

$$p = \frac{\sum_{i=1}^{n} V_i}{V^{RVE}}, \tag{9}$$

where R_i and V_i are the radii and volumes of individual pores and n is the number of pores in RVE. For oblate spheroidal pores with semi-axes $a_1 = a_2 = R$, $a_3 = \alpha \cdot R$, these two measures of defect density are related by a scalar multiplier: $\rho = \frac{3}{4\pi\alpha} p$. The results for the ideal flat penny-shaped crack are obtained when $\alpha \to 0$.

3.2. Model preparation and post-processing of results

The effective stiffness or compliance tensors of a heterogeneous material represent sets of proportionality coefficients relating macroscopic averages of stress and strain within the considered RVE. It was shown that, for RVEs containing finite number of inhomogeneities, homogenization based on prescribing uniform strains on the boundaries overestimates the overall stiffness while prescribing uniform stresses results in underestimation of it, see discussion in Suquet (1987), Huet (1990) and Hazanov and Huet (1994). Suquet (1987) also proved that application of periodic boundary conditions results in effective stiffness predictions which are bounded by the properties obtained based on prescribing the uniform stresses and the uniform strains. For the microstructures considered in Suquet (1987), the numerical results obtained using periodic boundary conditions were in better agreement with experimental results than the uniform ones.

In this work, we utilize periodic RVEs subjected to periodic boundary conditions implemented in displacements. Formulation of the boundary conditions can be found in Xia et al. (2003) and Segurado and Llorca (2002); the numerical implementation of the these conditions in MSC Marc Mentat is described in Drach et al. (2014,2016) and Trofimov et al. (2017).

Simulations for six loadcases are performed on each RVE. Each loadcase consists of a set of boundary conditions in displacements corresponding to either a uniaxial tension in one of the directions of the global coordinate system or a simple shear. Based on the matrix material properties and distribution of the pores, the resulting material is orthotropic. Processing of the simulation results yields three Young's moduli along the global coordinate axes, three shear moduli and three Poisson's ratios. All FEA model preparation steps are automated *via* a custom script which assigns material properties, boundary conditions and creates load cases (see Drach et al., 2016 for details). The average strains applied in each load case are chosen to be small so the initial volumes of the finite elements are not changed significantly and remain suitable for the volume averaging procedure. A custom Python script described in Drach et al. (2016) is used to calculate the effective stiffness tensor components of the RVEs.

3.3. Mesh parameters' studies

The RVEs used in this research are meshed with tetrahedral elements. The effects of element types and mesh density are investigated for representative implementation of the RVE with cracks modeled as strongly oblate spheroids with aspect ratio $\alpha = 0.01$ (penny-shaped cracks) and crack density $\rho = 0.35$. The parametric studies were performed for orthotropic material with the following parameters: E_1=1, E_2=2, E_3=5, G_{12}=1.3, G_{23}=2.5, G_{13}=4, ν_{12}=0.2, ν_{23}=0.14, ν_{13}=0.05.

To evaluate the effect of mesh type, we compared predictions obtained for the RVE meshed with 1,960,638 linear tetrahedral (tetra4, Marc ID# 134) and the same number of quadratic tetrahedral (tetra10, Marc ID# 127) elements. In this test model, the observed percentage difference did not exceeded 1.81%, see Table 1. Due to the small difference between linear and quadratic element mesh predictions and considerably higher computational cost of the simulations using quadratic elements, the linear tetrahedral elements were utilized in all subsequent simulations.

A parametric study was conducted to evaluate the accuracy of the model as a function of the number of elements. Two mesh refinement strategies were utilized: uniform reduction of the element size and mesh refinement at the crack tips. Figs. 2 and 3 show how the predictions of effective elastic properties converge with refinement of the mesh at the crack tips to the values obtained with approximately uniform mesh of 6 million elements. The solid line is obtained by quadratic interpolation of the data points (denoted by "×") produced by utilizing the mesh refinement at the crack tips. Table 2 shows that the relative difference for all material constants (MC) calculated as

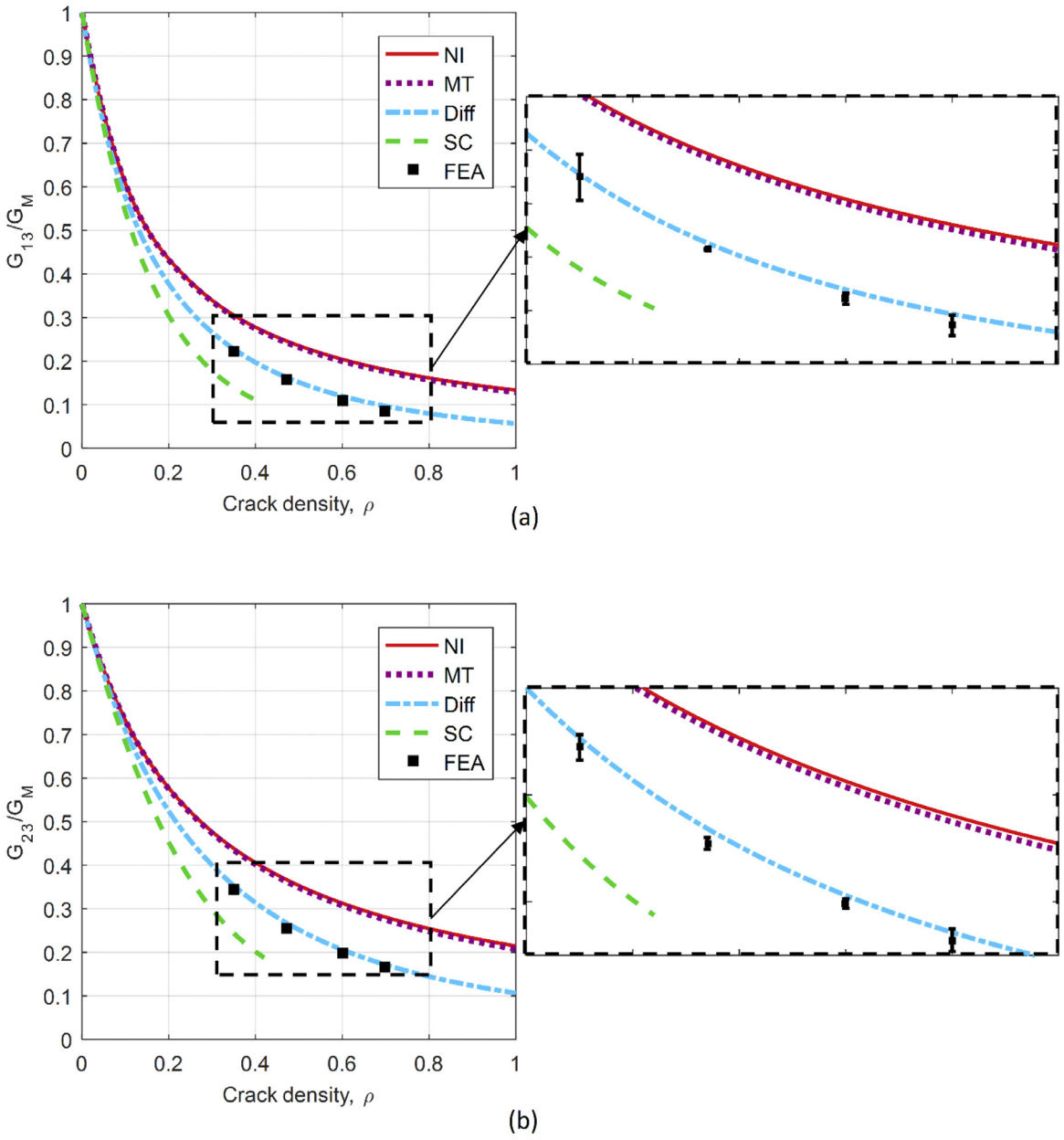

Fig. 6. Out-of-plane shear moduli (a) G_{13} and (b) G_{23} for orthotropic material with parallel cracks.

Table 1
Comparison of elastic moduli predictions obtained using two element types: linear and quadratic. The relative difference is calculated as $\delta = \frac{linear-quadratic}{uncracked} \cdot 100\%$.

	E_2/E_{2M}	E_3/E_{3M}	E_1/E_{1M}	G_{23}/G_{23M}	G_{13}/G_{13M}	G_{12}/G_{12M}	v_{23}/v_{23M}	v_{31}/v_{31M}	v_{21}/v_{21M}
Linear	0.9853	0.2417	0.9854	0.3587	0.2560	0.9852	1.0268	0.2588	0.9998
Quadratic	0.9853	0.2235	0.9854	0.3434	0.2442	0.9852	1.0305	0.2408	0.9998
δ, %	0	1.81	0	1.53	1.18	0	0.37	1.79	0

Table 2
Percentage difference between effective elastic constants (MC) predicted by FE model with 2 and 6 million finite elements.

MC	E2	E3	E1	G23	G13	G12	v23	v31	v21
δ, %	0.01	3.44	0.01	2.04	1.99	0.01	0.18	3.15	0

$\delta = \frac{MC^{(2\ mln.)} - MC^{(6\ mln.)}}{MC^{(6\ mln.)}} 100\%$ does not exceed 3.44%. The RVEs with approximately 2 mln. are used in the subsequent simulations.

4. Prediction of effective elastic properties for orthotropic materials with cracks

A significant number of natural (rocks, wood) and man-made (ceramic coatings, laminated and woven) composites are not isotropic. In this section, we consider an orthotropic material with parallel penny-shaped crack-like pores. We assume the pores to be parallel to one of the material orthotropy planes, but the approach is readily applicable to any orientation of pores in the material. To perform comparison of the micromechanical schemes with the

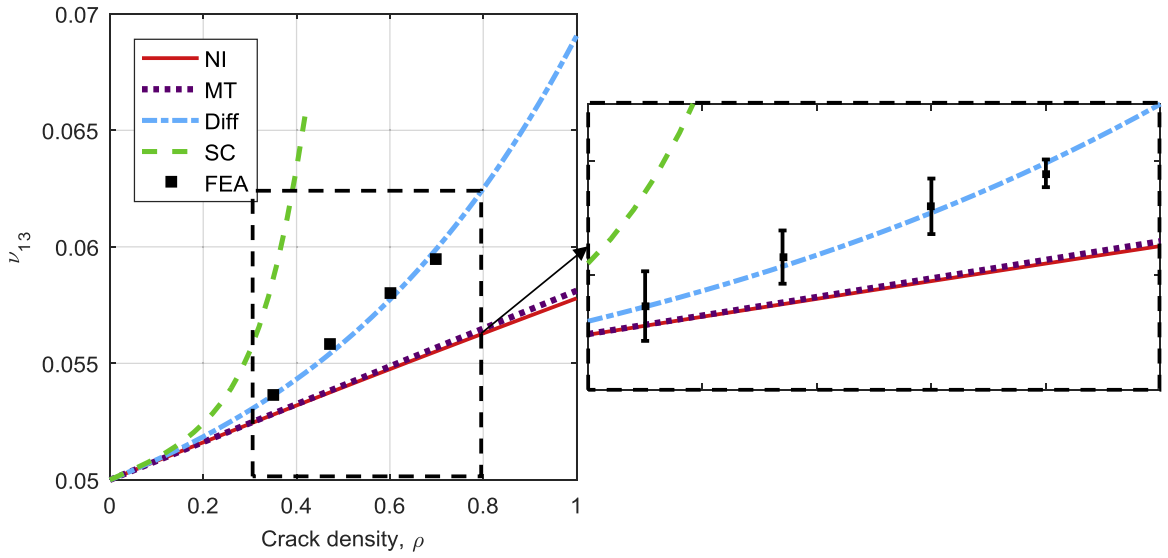

Fig. 7. Poisson's ratio ν_{13} for orthotropic material with parallel cracks.

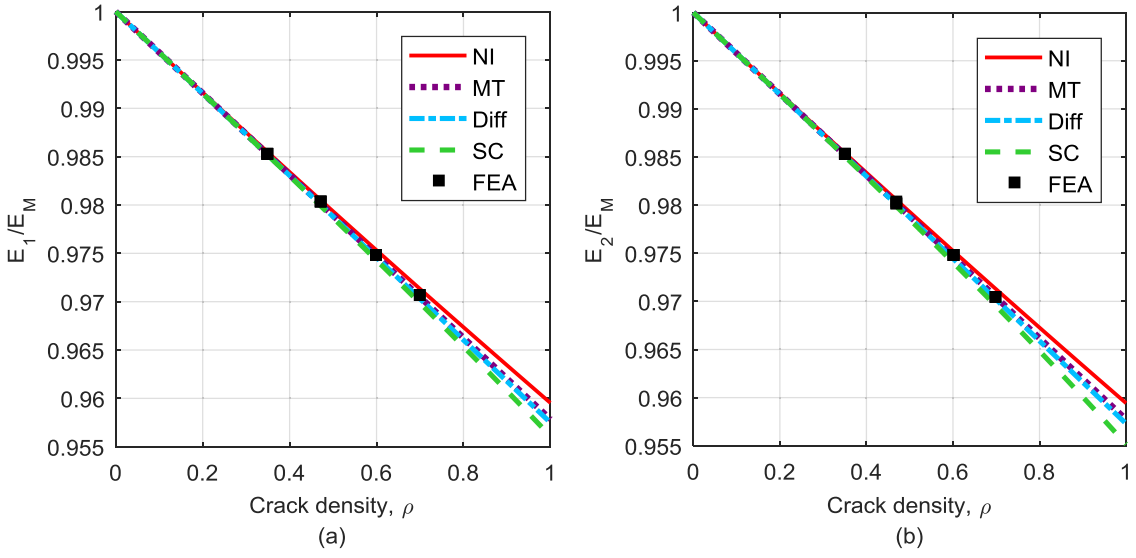

Fig. 8. In-plane Young's moduli (a) E_1 and (b) E_2 for orthotropic material with parallel cracks.

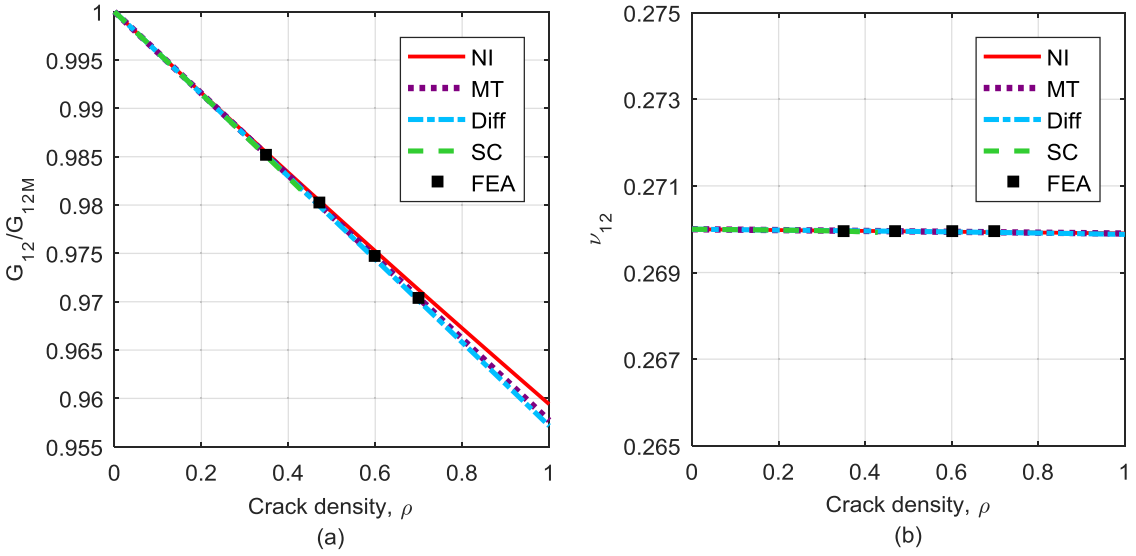

Fig. 9. (a) In-plane shear modulus and (b) in-plane Poisson's ratio for orthotropic material with parallel cracks.

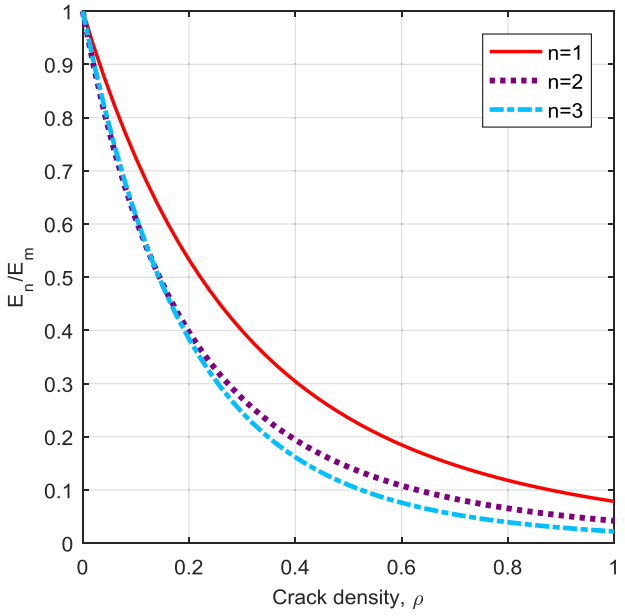

Fig. 10. Young's moduli E_n in principal material directions $n = 1,2,3$ when cracks are normal to those directions.

direct FEA simulations, we need to use the components of the Eshelby tensor. We start with the discussion of the procedure to evaluate the Eshelby tensor components for an ellipsoidal inclusion in an orthotropic matrix.

4.1. Validation of Gaussian quadrature procedure for components of Eshelby tensor

The expressions for components of the Eshelby tensor for spheroidal inclusion were obtained in a closed analytical form up to the transversely isotropic symmetry of a material (Kanaun and Levin, 1994; Sevostianov et al., 2005). The Eshelby solution for the material with more general anisotropy is only achievable numerically. The approach utilizing Gaussian quadratures was proposed by Ghahremani (1977) and Gavazzi and Lagoudas (1990). We use the expressions for components of Eshelby tensor provided in

Table 3
Matrix representation of the fourth rank Eshelby tensor.

s_{1111}	s_{1122}	s_{1133}	s_{1123}	s_{1131}	s_{1112}
s_{2211}	s_{2222}	s_{2233}	s_{2223}	s_{2231}	s_{2212}
s_{3311}	s_{3322}	s_{3333}	s_{3323}	s_{3331}	s_{3312}
s_{2311}	s_{2322}	s_{2333}	s_{2323}	s_{2331}	s_{2312}
s_{3111}	s_{3122}	s_{3133}	s_{3123}	s_{3131}	s_{3112}
s_{1211}	s_{1222}	s_{1233}	s_{1223}	s_{1231}	s_{1212}

Kirilyuk et al. (2007) for the case of orthotropic material:

$$s_{ijmn}{}^{(\alpha,\beta,\gamma)} = \frac{1}{8\pi} C_{pqmn}^{(\alpha,\beta,\gamma)} \int_{-1}^{1} \int_{0}^{2\pi} \left(\tilde{G}_{ipjq}^{(\alpha,\beta,\gamma)}\left(\vec{\eta}\right) + \tilde{G}_{jpiq}^{(\alpha,\beta,\gamma)}\left(\vec{\eta}\right) d\omega \right) d\xi_3, \tag{10}$$

where

$$\tilde{G}_{ijkl}^{(\alpha,\beta,\gamma)} = \bar{\eta}_k \bar{\eta}_l \left(K_{ij}\left(\vec{\eta}\right) \right)^{-1} \bar{\eta}_i = \frac{\xi_i}{a_i}, \ \xi_1 = \sqrt{1-\xi_3{}^2}\cos\omega,$$

$$\xi_2 = \sqrt{1-\xi_3{}^2}\sin\omega, \ K_{ki}\left(\vec{\xi}\right) = C_{kjil}^{(\alpha,\beta,\gamma)} \xi_j \xi_l,$$

a_i is the length of the ith axis of the ellipsoidal inhomogeneity and $C_{kjil}^{(\alpha,\beta,\gamma)}$ is the stiffness tensor of an orthotropic material in the coordinate system of the ellipsoid. Angles α, β and γ are the Euler's angles for the material symmetry axes X_i $(i = 1,2,3)$ in the coordinate system x_i of the ellipsoid, see Fig. 4.

In order to check the validity of our numerical evaluation of (10) implemented in the Gaussian quadratures, a comparison between our results and the available theoretical solutions was performed. For transversely isotropic matrix material with co-axial transversely isotropic inhomogeneities, the theoretical solution is given by Sevostianov et al. (2005). In the comparison, we represented the crack as a strongly oblate spheroid with aspect ratio $\alpha = 0.01$ and assumed it to be parallel to the plane of isotropy X_1-X_2. The material properties are E_3=5, E_1=2, ν_{12}=0.14, ν_{13}=0.3, G_{32}=4. Arranging components of the fourth rank Eshelby tensor **s** in the matrix form (as shown in Table 3), the analytical predictions of the components are given in Table 4. Comparing them with the Gaussian quadrature evaluation presented in Table 5, we observe that the largest relative error between the components is 2.75%.

For orthotropic matrix material, there is no analytical solution of the Eshelby problem in the three dimensional case. However,

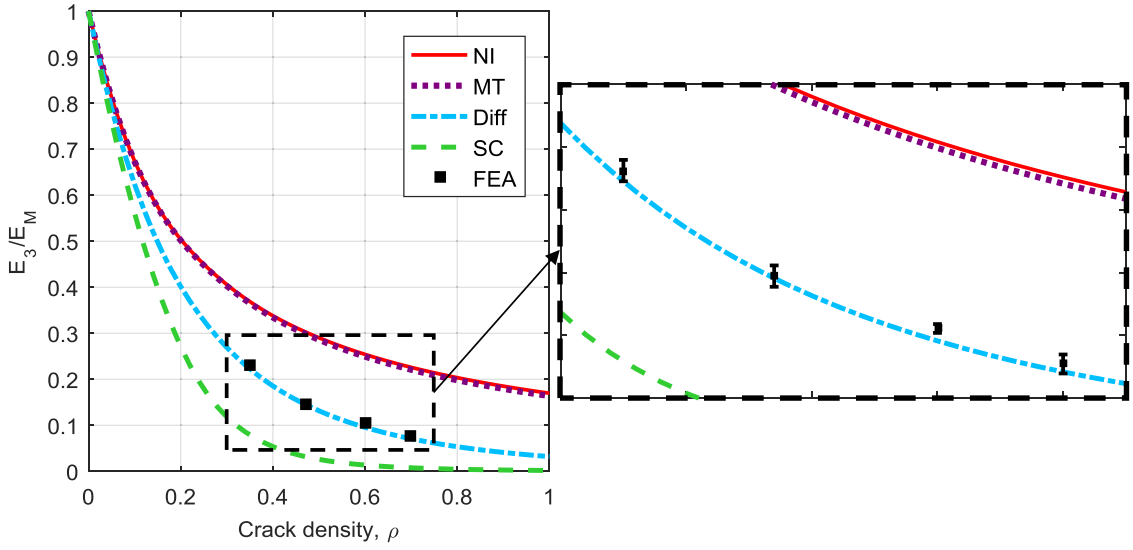

Fig. 11. Out-of-plane Young's modulus for isotropic material with parallel cracks.

Table 4
The components of Eshelby tensors obtained analytically using the solution proposed by Sevostianov et al. (2005).

6.1997E−03	−4.2076E−04	−2.9813E−03	0	0	0
−4.2076E−04	6.1997E−03	−2.9813E−03	0	0	0
3.4420E−01	3.4420E−01	9.9647E−01	0	0	0
0	0	0	4.9613E−01	0	0
0	0	0	0	4.9613E−01	0
0	0	0	0	0	3.3102E−03

Table 5
The components of Eshelby tensors obtained numerically using Gaussian quadratures.

6.1993E−03	−4.0918E−04	−2.9330E−03	0	0	0
−4.0918E−04	6.1993E−03	−2.9330E−03	0	0	0
3.4421E−01	3.4421E−01	9.9643E−01	0	0	0
0	0	0	4.9614E−01	0	0
0	0	0	0	4.9614E−01	0
0	0	0	0	0	3.3042E−03

Table 6
Comparison of H-tensor components for orthotropic matrix material.

	H_{1111}	H_{1122}	H_{2222}	H_{1212}
Analytical	1.0005E+00	−6.8524E−01	9.0555E+01	1.3153E+02
Numerical	1.0129E+00	−6.8476E−01	9.3398E+01	1.3231E+02
δ, %	1.24	0.07	3.14	0.59

the analytical solution in 2D for the elliptic holes can be found in Tsukrov and Kachanov (2000). Assuming that the principal material axes X_1-X_2 coincide with the axes of ellipse, they provide expressions for components of compliance contribution tensor H_{1111}, H_{1122}, H_{1212}, and H_{2222}. For validation of our numerical procedure we compare the numerical results for a strongly elongated flat ellipsoid having semi axes 1: 0.01: 1000 with the plane strain analytical solution. The engineering constants of the matrix are E_1=1, E_2=2, E_3=5, G_{12}=1.3, G_{23}=2.5, G_{13}=4, ν_{12}=0.2, ν_{23}=0.14, ν_{13}=0.05. Both the 2D elliptic holes and 3D ellipsoidal pores are perpendicular to X_2 direction. In the 3D numerical results, the compliance contribution tensor **H** is calculated from formula (2) using the components of Eshelby tensor (10).

Table 6 shows the comparison between **H**-tensor components obtained using analytical solution of Tsukrov and Kachanov (2000) and the numerical solution given by formulas (2) and (10) and implemented using Gaussian quadratures. The largest relative error $\delta = \frac{|H_{ijkl}^{Analyt.} - H_{ijkl}^{Numer.}|}{H_{ijkl}^{Analyt.}}$, $(i, j, k, l = 1, 2)$, between the components is 3.14%. Note that we obtained numerically *all* components of **H**, but present only the data needed for comparison and validation of our Gaussian integration procedure.

4.2. Evaluation of micromechanical schemes for cracks in an orthotropic matrix

In this section, the effective elastic properties of the orthotropic material containing parallel crack-like penny-shaped pores are presented as functions of the crack density ρ. The micromechanical models are implemented using numerically calculated Eshelby tensor (10). The differential, Mori–Tanaka, self-consistent and non-interaction schemes are considered. The orthotropic material is chosen to have its stiffest direction perpendicular to the cracks. All cracks within each representative volume element are of the same shape and size. At least three realizations were considered for each value of crack density in order to obtain the standard deviation error bars. The elastic constants and Poisson's ratios of the considered material are the same as in the parametric mesh studies (Section 3) E_1=1, E_2=2, E_3=5, G_{12}=1.3, G_{23}=2.5, G_{13}=4, ν_{12}=0.2, ν_{23}=0.14, ν_{13}=0.05, and all of the cracks are parallel to the X_1-X_2 plane.

The micromechanical modeling predictions are compared to the direct FEA simulation results for the values of crack density $\rho = 0.35, 0.47, 0.6, 0.7$, see Figs. 5–9. As seen in the figures, the overall out-of-plane properties E_3, G_{23}, G_{13} ν_{13} are better predicted by the differential scheme. Thus, our observations are similar to these of Saenger et al. (2006) made for cracks in isotropic matrix. Also, as discussed in the literature, the non-interaction and Mori–Tanaka predictions practically coincide for slightly inflated cracks (they become identical for perfectly flat cracks with $\alpha = 0$).

As shown in Figs. 8 and 9, for the in-plane properties E_1, E_2, G_{12} and ν_{12}, the reduction in stiffness is caused by the fact that the cracks are presented as strongly oblate spheroids with $\alpha = 0.01$. These small reductions appear to be better reproduced by the Mori–Tanaka scheme. Note that for completely flat penny-shaped cracks with $\alpha = 0$, there would be no influence on in-plane elastic moduli.

The self-consistent micromechanical model seems to significantly underpredict the effective stiffness of the material as was previously noted, for example, in Kachanov et al. (1994). According to SCS, the material's stiffness approaches zero when the crack density reaches approximately $\rho = 0.4$, so it becomes impossible to calculate the effective properties of a material with a higher crack density utilizing this scheme. This explains why the corresponding curves interrupt at $\rho = 0.4$ in Figs. 5–7.

Analysis of Fig. 6 shows that there is a difference in the reduction of the out-of-plane effective shear moduli due to the material anisotropy. Even though each crack is represented by a spheroid which is symmetric in X_1-X_2 plane, the difference between the predictions of shear moduli G_{13} and G_{23} is observed. In particular, G_{13} decreases faster with increase in the crack density than G_{23} which can be explained by the fact that the stiffness in the matrix material's first direction is lower than in the second. This observation indicates that in an orthotropic material, the aligned axisymmetric defects affect the overall stiffness in different directions differently due to the anisotropy of the matrix material.

Fig. 10 shows contributions of aligned cracks to the effective Young's moduli predicted by the differential scheme when the cracks are normal to each of the principal material directions. It can be seen that the reduction in the effective moduli due to the presence of the cracks depends on the orientation of the cracks with respect to the principal material directions. Cracks perpendicular to the stiffer direction produce greater relative reduction in the effective stiffness compared to cracks perpendicular to the softer direction. These results are consistent with the observa-

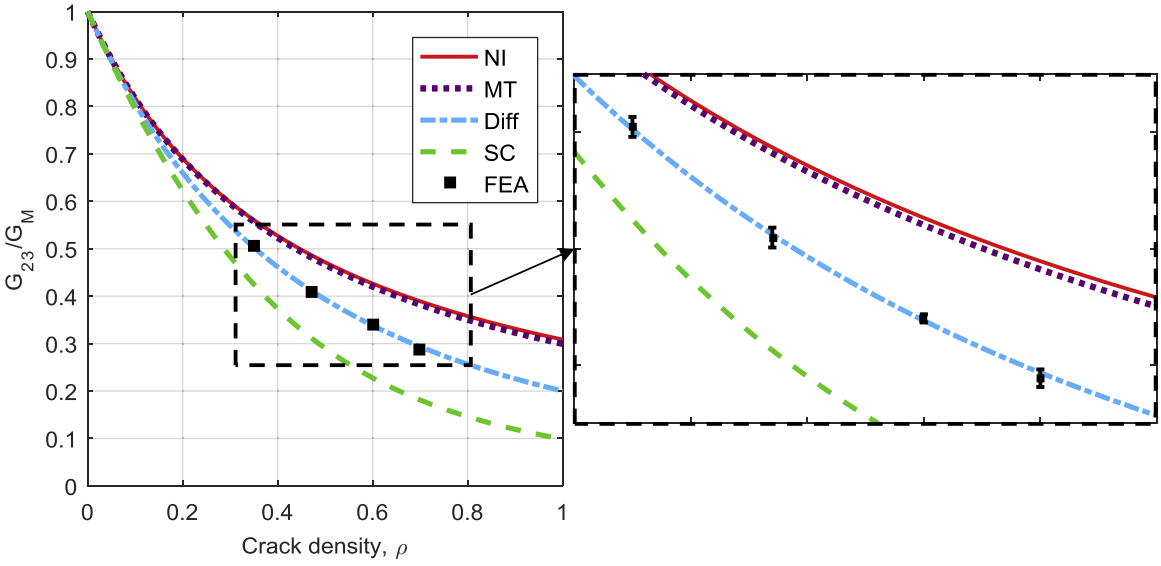

Fig. 12. Out-of-plane shear modulus for isotropic material with parallel cracks.

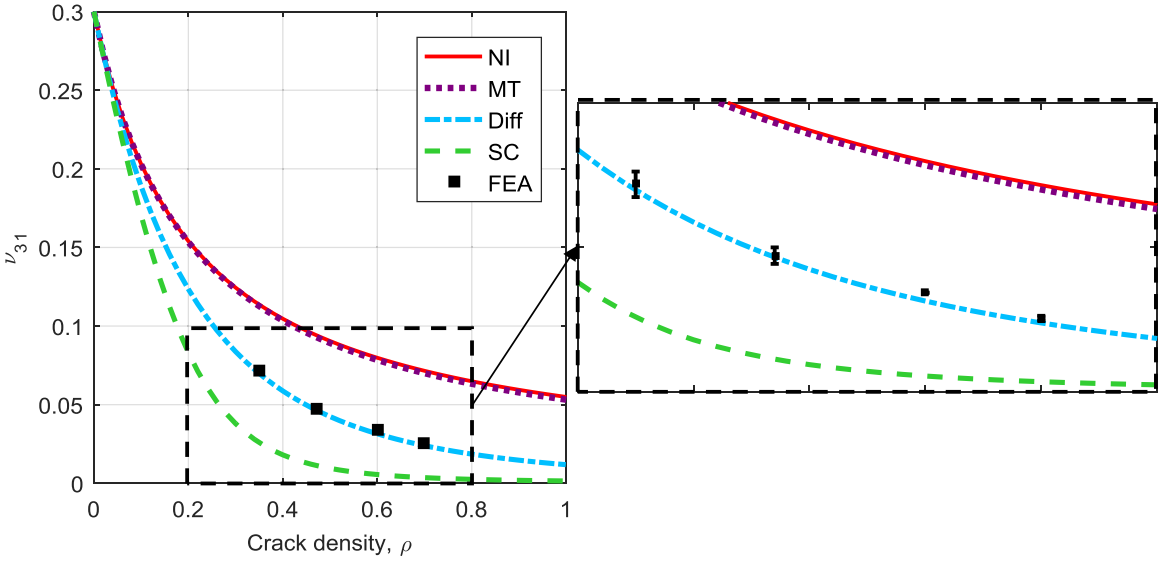

Fig. 13. Poisson's ratio for isotropic material with parallel cracks.

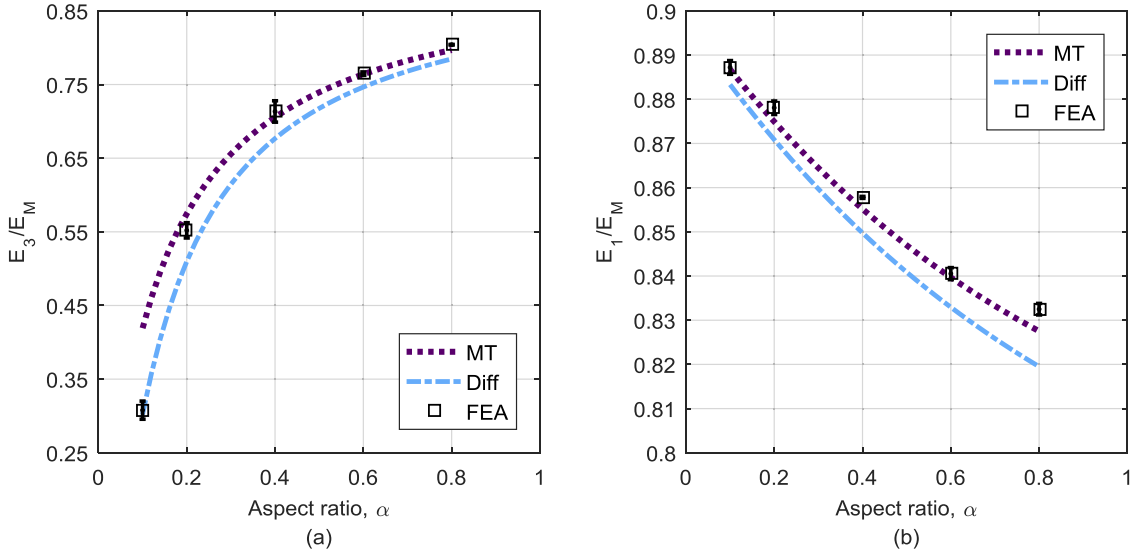

Fig. 14. Variation of (a) out-of-plane and (b) in-plane Young's moduli with the pore aspect ratio for porosity $p = 0.1$.

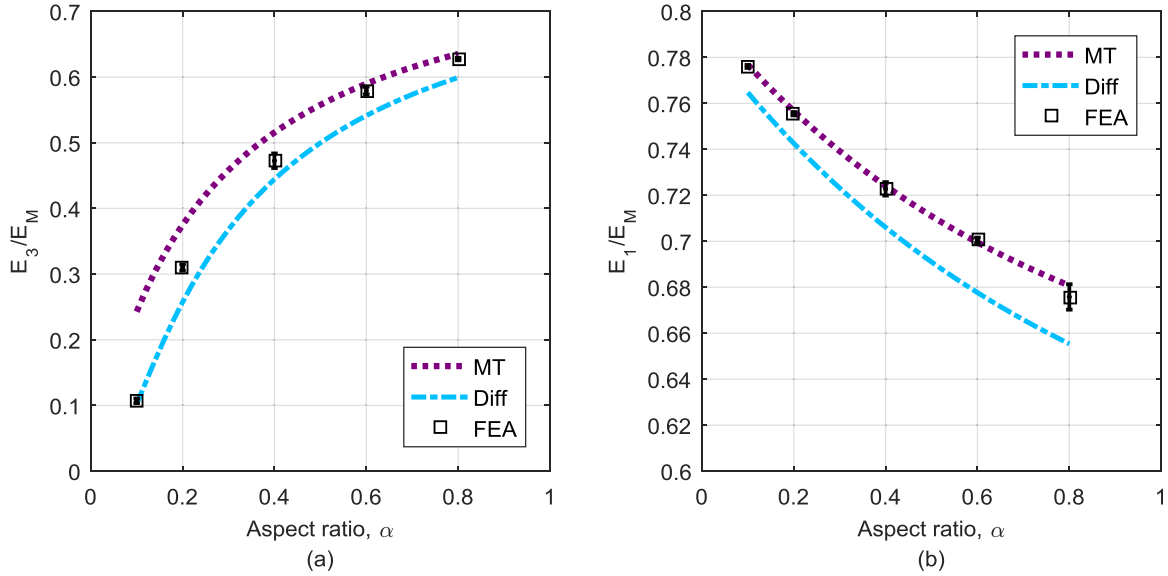

Fig. 15. Variation of (a) out-of-plane and (b) in-plane Young's moduli with the pore aspect ratio for porosity $p = 0.2$.

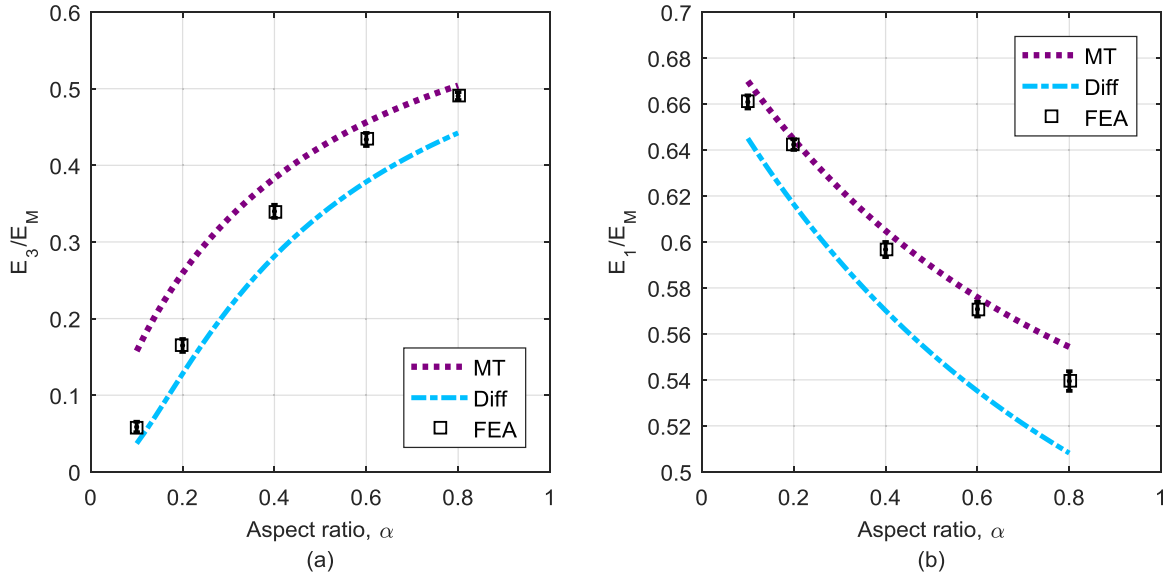

Fig. 16. Variation of (a) out-of-plane and (b) in-plane Young's moduli with the pore aspect ratio for porosity $p = 0.3$.

tions reported in Mauge and Kachanov (1994) and Tsukrov and Kachanov (2000).

5. Evaluation of micromechanical schemes for inflated cracks in isotropic material

As shown in the previous section, the best predictions for the effective out-of-plane properties of the orthotropic material with parallel penny-shaped crack-like pores ($\alpha \approx 0$) is given by the differential micromechanical scheme. Numerical simulations show that the differential scheme also provides the best agreement with the direct FEA simulations in the case of the isotropic matrix, see Figs. 11–13. However, for spherical ($\alpha = 1$) and spheroidal ($\alpha = 2$) pores, the Mori–Tanaka scheme is more accurate, see Drach et al. (2016). In this section we determine the value of the aspect ratio α at which predictions for the out-of-plane moduli by the Mori–Tanaka scheme become closer to the FEA results than the differential scheme. We compare the FEA results with micromechanical predictions for Young's moduli E_3 and E_1 as functions of the aspect ratio α for the porosity levels $p = 0.1$, 0.2, 0.3. The results are presented in Figs. 14–16.

As can be seen, the in-plane Young's modulus is better predicted by Mori–Tanaka scheme for all considered aspect ratios. However, the best choice of the micromechanical scheme for the out-of-plane Young's modulus E_3 depends on the pores' aspect ratio. As we go from the crack-like to the inflated pores, the differential scheme becomes less accurate than Mori–Tanaka. The transition happens at $\alpha \approx 0.2$ for $p = 0.1$, and $\alpha \approx 0.4$ for $p = 0.2$ and 0.3.

6. Conclusions

In this paper we employed FEA of periodic RVEs to evaluate the accuracy of several popular micromechanical schemes in predicting the effective elastic properties of solids with randomly distributed penny-shaped cracks in the orthotropic matrix. The cracks were represented as oblate spheroidal pores having aspect ratio $\alpha = 0.01$. Periodic RVEs were generated utilizing an efficient implementation

of the RSA algorithm suitable for numerical analysis. The FE models with curvature-dependent conforming finite element meshes were developed. Several realizations of RVEs for each crack density were analyzed.

The considered micromechanical schemes included the non-interaction approximation, self-consistent, differential, and Mori–Tanaka. They were implemented using the compliance contribution tensor based on the Eshelby solution. For isotropic and transversely isotropic matrix, the analytical expressions for the components of Eshelby tensors were utilized. In the case of orthotropic matrix, the components were calculated numerically via Gaussian quadratures of surface integrals.

For the considered combination of the material symmetry, defect shape and orientation, the differential micromechanical scheme was observed to provide the best agreement with the FEA results for the out-of-plane properties. This observation is similar to the predictions of Saenger et al. (2006) for cracks in isotropic matrix.

In addition, we investigated the accuracy of the micromechanical schemes as a function of the pore aspect ratio starting with a penny-shaped crack ($\alpha = 0.01$) up to a slightly deformed sphere ($\alpha = 0.8$). This study was conducted for parallel oblate spheroids in the isotropic matrix. A gradual transition from the differential to Mori–Tanaka as the "best" scheme in the case of the out-of-plane properties was observed with increasing α. This result is consistent with previous publications (see, for example, Drach et al., 2016), in which it was demonstrated that for mildly prolate spheroidal and spherical pores, the Mori–Tanaka scheme is in the best agreement with direct FEA. The in-plane elastic constants can be predicted by the Mori–Tanaka scheme for all the considered aspect ratios α with good accuracy.

Acknowledgments

This material is based upon work supported by the National Science Foundation through grant CMMI-1662098. The second author, B.D., also acknowledges the financial support from the New Mexico Space Grant Consortium through NASA Cooperative Agreement NNX15AK41A.

References

Benveniste, Y., 1987. A new approach to the application of Mori–Tanaka's theory in composite materials. Mech. Mater. 6 (2), 147–157. doi:10.1016/0167-6636(87)90005-6.

Budiansky, B., 1965. On the elastic moduli of some heterogeneous materials. J. Mech. Phys. Solids 13 (4), 223–227. doi:10.1016/0022-5096(65)90011-6.

Dahm, T., Becker, T.W., 1998. On the elastic and viscous properties of media containing strongly interacting in-plane cracks. Pure Appl. Geophys. 151 (1), 1–16. doi:10.1007/s000240050102.

Deng, H., Nemat-Nasser, S., 1992. Microcrack arrays in isotropic solids. Mech. Mater. 13 (1), 15–36. doi:10.1016/0167-6636(92)90033-A.

Drach, A., Drach, B., Tsukrov, I., 2014. Processing of fiber architecture data for finite element modeling of 3D woven composites. Adv. Eng. Software 72, 18–27. doi:10.1016/j.advengsoft.2013.06.006.

Drach, B., Tsukrov, I., Trofimov, A., 2016. Comparison of full field and single pore approaches to homogenization of linearly elastic materials with pores of regular and irregular shapes. Int. J. Solids Struct. 96, 48–63. doi:10.1016/j.ijsolstr.2016.06.023.

Eroshkin, O., Tsukrov, I., 2005. On micromechanical modeling of particulate composites with inclusions of various shapes. Int. J. Solids Struct. 409–427. doi:10.1016/j.ijsolstr.2004.06.045.

Eshelby, J.D., 1957. The determination of the elastic field of an ellipsoidal inclusion, and related problems. Proc. R. Soc. A: Math. Phys. Eng. Sci. 241 (1226), 376–396. doi:10.1098/rspa.1957.0133.

Gavazzi, A.C., Lagoudas, D.C., 1990. On the numerical evaluation of Eshelby's tensor and its application to elastoplastic fibrous composites. Comput. Mech. 7 (1), 13–19. doi:10.1007/BF00370053.

Ghahremani, F., 1977. Numerical evaluation of the stresses and strains in ellipsoidal inclusions in an anisotropic elastic material. Mech. Res. Commun. 4 (2), 89–91. doi:10.1016/0093-6413(77)90018-0.

Gottesman, T., Hashin, Z., Brull, M.A., 1980. Effective Elastic Moduli of Cracked Fiber Composites. In: Advances in Composite Materials. Elsevier, pp. 749–758. doi:10.1016/B978-1-4832-8370-8.50061-9.

Grechka, V., 2007. Comparison of the non-interaction and differential schemes in predicting the effective elastic properties of fractured media. Int. J. Fract. 144 (3), 181–188. doi:10.1007/s10704-007-9088-z.

Grechka, V., Kachanov, M., 2006. Effective elasticity of rocks with closely spaced and intersecting cracks. Geophysics 71 (3), D85–D91. doi:10.1190/1.2197489.

Hashin, Z., 1988. The differential scheme and its application to cracked materials. J. Mech. Phys. Solids 36 (6), 719–734. doi:10.1016/0022-5096(88)90005-1.

Hashin, Z., Shtrikman, S., 1963. A variational approach to the theory of the elastic behaviour of multiphase materials. J. Mech. Phys. Solids 11 (2), 127–140. doi:10.1016/0022-5096(63)90060-7.

Hazanov, S., Huet, C., 1994. Order relationships for boundary conditions effect in heterogeneous bodies smaller than the representative volume. J. Mech. Phys. Solids 42 (12), 1995–2011. doi:10.1016/0022-5096(94)90022-1.

Hill, R., 1963. Elastic properties of reinforced solids: Some theoretical principles. J. Mech. Phys. Solids 11 (5), 357–372. doi:10.1016/0022-5096(63)90036-X.

Hill, R., 1965. A self-consistent mechanics of composite materials. J. Mech. Phys. Solids 13 (March 1962), 213–222. doi:10.1016/0022-5096(65)90010-4.

Horii, H., Nemat-Nasser, S., 1983. Overall moduli of solids with microcracks: load-induced anisotropy. J. Mech. Phys. Solids 31 (2), 155–171. doi:10.1016/0022-5096(83)90048-0.

Huet, C., 1990. Application of variational concepts to size effects in elastic heterogeneous bodies. J. Mech. Phys. Solids 38 (6), 813–841. doi:10.1016/0022-5096(90)90041-2.

Kachanov, M., 1993. Elastic Solids with Many Cracks and Related Problems, pp. 259–445. doi:10.1016/S0065-2156(08)70176-5.

Kachanov, M.L., 1987. Elastic solids with many cracks: a simple method of analysis. Int. J. Solids Struct. 23 (1), 23–43. doi:10.1016/0020-7683(87)90030-8.

Kachanov, M., Tsukrov, I., Shafiro, B., 1994. Effective moduli of solids with cavities of various shapes. Appl. Mech. Rev. 47 (1S), S151. doi:10.1115/1.3122810.

Kanaun, S.K., Levin, V.M., 1994. Effective Field Method in Mechanics of Matrix Composite Materials. In: Recent Advances in Mathematical Modelling of Composite Materials. World Scientific Publishing, Singapore, pp. 1–58.

Kirilyuk, V.S., Levchuk, O.I., Tkachenko, V.F., 2007. On the static equilibrium of an elastic orthotropic medium with an arbitrarily oriented elliptical crack. Strength Mater. 39 (4), 443–453. doi:10.1007/s11223-007-0050-0.

Kröner, E., 1958. Berechnung der elastischen konstanten des vielkristalls aus den konstanten des einkristalls. Z. Phys. 151 (4), 504–518. doi:10.1007/BF01337948.

Kushch, V.I., Sevostianov, I., 2004. Effective elastic properties of the particulate composite with transversely isotropic phases. Int. J. Solids Struct. 41 (3–4), 885–906. doi:10.1016/j.ijsolstr.2003.09.001.

Laws, N., Dvorak, G.J., Hejazi, M., 1983. Stiffness changes in unidirectional composites caused by crack systems. Mech. Mater. 2 (2), 123–137. doi:10.1016/0167-6636(83)90032-7.

Markov, K.Z., 1999. Elementary micromechanics of heterogeneous media. Heterogen. Media: Modell. Simul. 1–162. doi:10.1007/978-1-4612-1332-1_1.

Mauge, C., Kachanov, M., 1994. Effective elastic properties of an anisotropic material with arbitrarily oriented interacting cracks. J. Mech. Phys. Solids 42 (4), 561–584. doi:10.1016/0022-5096(94)90052-3.

McLaughlin, R., 1977. A study of the differential scheme for composite materials. Int. J. Eng. Sci. 15 (4), 237–244. doi:10.1016/0020-7225(77)90058-1.

Mori, T., Tanaka, K., 1973. Average stress in matrix and average elastic energy of materials with misfitting inclusions. Acta Metall. 21 (5), 571–574. doi:10.1016/0001-6160(73)90064-3.

Mura, T., 1987. Micromechanics of defects in solids. Mech. Elast. Inelast. Solids doi:10.1007/s13398-014-0173-7.2.

Orlowsky, B., Saenger, E.H., Guéguen, Y., Shapiro, S.A., 2003. Effects of parallel crack distributions on effective elastic properties - a numerical study. Int. J. Fract. 124 (3/4), L171–L178. doi:10.1023/B:FRAC.0000022563.29991.80.

Rintoul, M.D., Torquato, S., 1997. Reconstruction of the structure of dispersions. J. Colloid Interface Sci. 186 (2), 467–476. doi:10.1006/jcis.1996.4675.

Saenger, E.H., 2007. Comment on 'comparison of the non-interaction and differential schemes in predicting the effective elastic properties of fractured media' by V. Grechka. Int. J. Fract. 146 (4), 291–292. doi:10.1007/s10704-007-9138-6.

Saenger, E.H., Krüger, O.S., Shapiro, S.A., 2006. Effective elastic properties of fractured rocks: dynamic vs. static considerations. Int. J. Fract. 139 (3–4), 569–576. doi:10.1007/s10704-006-0105-4.

Salganik, R.L., 1973. Mechanics of bodies with a large numbers of cracks. Mech. Solids 4, 149–158.

Seelig, T., Rafiee, S., Gross, D., 2000. Simple method for the investigation of elastic bodies of finite size containing many cracks. Int. J. Eng. Sci. 38 (13), 1459–1472. doi:10.1016/S0020-7225(99)00117-2.

Segurado, J., Llorca, J., 2002. A numerical approximation to the elastic properties of sphere-reinforced composites. J. Mech. Phys. Solids 50 (10), 2107–2121. doi:10.1016/S0022-5096(02)00021-2.

Sevostianov, I., Kachanov, M., 2002. Explicit cross-property correlations for anisotropic two-phase composite materials. J. Mech. Phys. Solids 50 (2), 253–282. doi:10.1016/S0022-5096(01)00051-5.

Sevostianov, I., Yilmaz, N., Kushch, V., Levin, V., 2005. Effective elastic properties of matrix composites with transversely-isotropic phases. Int. J. Solids Struct. 42 (2), 455–476. doi:10.1016/j.ijsolstr.2004.06.047.

Suquet, P.M., 1987. Elements of Homogenization for Inelastic Solid Mechanics. In: Homogenization Techniques for Composite Media. Springer-Verlag, pp. 193–278.

Trofimov, A., Drach, B., Sevostianov, I., 2017. Effective elastic properties of composites with particles of polyhedral shapes. Int. J. Solids Struct. 120, 157–170. doi:10.1016/j.ijsolstr.2017.04.037.

Tsukrov, I., Kachanov, M., 2000. Effective moduli of an anisotropic material with elliptical holes of arbitrary orientational distribution. Int. J. Solids Struct. 37 (41), 5919–5941. doi:10.1016/S0020-7683(99)00244-9.

Willis, J.R., 1977. Bounds and self-consistent estimates for the overall properties of anisotropic composites. J. Mech. Phys. Solids 25 (3), 185–202. doi:10.1016/0022-5096(77)90022-9.

Withers, P.J.P., 1989. The determination of the elastic field of an ellipsoidal inclusion in a transversely isotropic medium, and its relevance to composite materials. Philos. Mag. A 59 (4), 759–781. doi:10.1080/01418618908209819.

Xia, Z., Zhang, Y., Ellyin, F., 2003. A unified periodical boundary conditions for representative volume elements of composites and applications. Int. J. Solids Struct. 40, 1907–1921. doi:10.1016/S0020-7683(03)00024-6.

Zimmerman, R.W., 1985. The effect of microcracks on the elastic moduli of brittle materials. J. Mater. Sci. Lett. 4 (12), 1457–1460. doi:10.1007/BF00721363.